

Symmetry deduction from spectral fluctuations in complex quantum systems

S. Harshini Tekur* and M. S. Santhanam†

Indian Institute of Science Education and Research, Dr. Homi Bhabha Road, Pune 411 008, India

The spectral fluctuations of complex quantum systems are known to be consistent with that from random matrices, but only for desymmetrized spectra. This implies that these fluctuations are affected by the discrete symmetries of the system. In this work, it is shown that the fluctuation characteristics and symmetry structure, for any arbitrary sequence of measured or computed levels, can be inferred from its higher-order spacing statistics without desymmetrization. In particular, for a spectrum composed of $k > 0$ independent sequences, its k -th order spacing ratio distribution is identical to its nearest neighbor counterpart with modified Dyson index k . This is demonstrated for random matrices, quantum billiards, spin chains and measured nuclear resonances with disparate symmetry features.

Spectral fluctuations in complex quantum systems are analyzed using the theoretical framework of random matrix theory (RMT) in many areas of physics [1–5]. These include few-body systems studied in quantum chaos [6] to interacting many-body systems in condensed matter [7], nuclear [8] and atomic physics [9]. These fluctuations carry signatures of the distinct phases observed in physical systems, *viz.*, integrable or chaotic limit of the underlying classical system [10], metallic or insulating phase [11], localized or thermal phase of many-body systems [12], low-lying shell model or mixing regime of nuclear spectra [13, 14].

Beginning with Wigner’s surmise [15] in the context of nuclear spectra, the present consensus is that spectral fluctuations of complex quantum systems, in suitable limit, display level repulsion consistent with that of an appropriately chosen ensemble of random matrices. For the special case of quantum chaotic systems, the Bohigas-Giannoni-Schmidt conjecture encapsulates this connection [16]. This has been amply verified in experiments [17], simulations [18] and derives some theoretical support based on semiclassical techniques [19].

Discrete symmetries of the system, *i.e.*, invariance of the potential under parity, reflection, rotations, are crucial in realizing this connection between spectral fluctuations and dynamical phases. In the presence of symmetries, the Hilbert space of the system splits into invariant subspaces or the Hamiltonian matrix H becomes block diagonal, *i.e.*, $H = H_1 \oplus H_2 \oplus \dots \oplus H_m$, with each block $H_i, i = 1, 2, \dots, m$ characterized by good quantum numbers corresponding to the respective symmetries [6]. To compute any measure of spectral fluctuation, all the discrete levels must be drawn from the same subspace.

If symmetries are ignored and levels from different blocks are superposed, the genuine correlation between levels (that might have produced level repulsion) is masked by near-degeneracies resulting in level clustering. This is misleading since this is also a spectral signature of integrable systems [20].

This implies that the level correlations are sensitive to the presence or absence of symmetries. It is then reasonable to expect the fluctuations of composite spectra,

superposed from many independent blocks, to contain information about the symmetry structure of the entire system. However, any measure based on the nearest neighbor (NN) fluctuations, such as the popular NN level spacing distribution, will always tend to the Poissonian limit (level clustering) due to the superposition of non-interacting blocks [21]. In this work, rigorous numerical evidence is presented to show that the higher-order level spacing ratio not only identifies the true fluctuation character, *viz.*, level clustering or repulsion, but also allows us to deduce quantitative information about the symmetry structure of the composite Hamiltonian matrix H .

This result effectively obviates the need for symmetry decomposition of quantum systems and also allows any arbitrary sequence of experimentally observed levels, whose symmetry structure is unknown, to be analyzed. This is of considerable interest in RMT as well [22]. Let G be a random matrix such that $G = G_1 \oplus G_2 \oplus \dots \oplus G_m$, a superposition of m blocks each of which is a Gaussian random matrix. If an arbitrary sequence of eigenvalues of G is given, the fluctuation properties and the block structure of G can be inferred from its higher-order fluctuation statistics. The proposed method is straightforward, involving only the calculation of spacing ratios. This is in contrast to the cumbersome methods proposed earlier based on two-level cluster function and requiring regression to deduce m from any composite spectrum [1, 2, 15, 23], all of which require unfolding as the first step.

Consider a sequence of eigenvalues $E_i, i = 1, 2, \dots, N$ of a quantum operator or a random matrix. Spectral fluctuations are relatively easier to analyze if spacing ratios defined as $r_i = \frac{E_{i+2} - E_{i+1}}{E_{i+1} - E_i}, i = 1, 2, \dots, N - 2$ are used instead of the spacings [24]. This is because the spacing ratios are independent of the local density of states and hence do not require spectral unfolding. For the case of the random matrix ensembles with Dyson index $\beta = 1, 2$ and 4, corresponding respectively to the Gaussian orthogonal, unitary and symplectic ensemble, the distribution

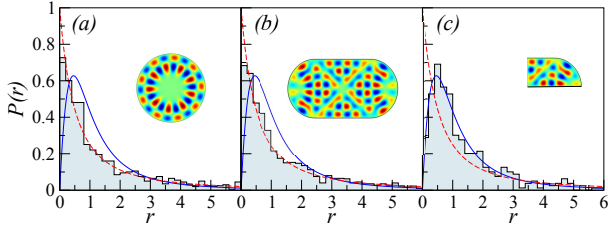


FIG. 1. Distribution $P(r)$ of the NN spacing ratios (histograms) for the circular (a), stadium (b) and desymmetrized stadium billiards (c). The broken (red) line represents $P_P(r)$ and the solid (blue) curve represents the Wigner surmise for ratios. The inset shows the shape of billiards and a typical eigenfunction superposed on it to emphasize its symmetry structure.

of spacing ratios is given by [25]

$$P(r, \beta) = C_\beta \frac{(r + r^2)^\beta}{(1 + r + r^2)^{1+3\beta/2}}. \quad (1)$$

For $\beta = 1$ these RMT models are applicable to Hamiltonians with time-reversal invariance, which will be the main focus of this paper. For integrable systems, the ratio distribution becomes $P_P(r) = 1/(1+r)^2$.

As motivation, in Fig. 1, the numerically computed distribution of NN spacing ratios $P(r)$ is shown for circular (integrable) [26] and stadium (chaotic) [27] billiards. The integrable billiards (Fig. 1(a)) expectedly agrees with $P_P(r)$. Note that stadium billiard has C_{2v} point group symmetry with four irreducible representations (irreps). If the spectra from each irrep is analyzed separately, by BGS conjecture, an agreement with $P(r, 1)$ of GOE is observed (Fig. 1(c)). However, in Fig. 1(b), the spectra from all the irreps is superposed, and hence the ratio distribution is closer to $P_P(r)$ with pronounced deviation from $P(r, 1)$. In such cases, as demonstrated below, true character of spectral fluctuations and the number m of independent spectra superposed can all be inferred using only the higher-order spacing ratio (HOSR) distributions without *a priori* knowledge of its symmetry structure.

To this end, we consider the non-overlapping k -th order spacing ratio, defined as

$$r_i^{(k)} = \frac{s_{i+k}^{(k)}}{s_i^{(k)}} = \frac{E_{i+2k} - E_{i+k}}{E_{i+k} - E_i}, \quad i, k = 1, 2, 3, \dots \quad (2)$$

In what follows, spectra from m independent blocks are superposed, and its distribution of k -th order spacing ratios is denoted by $P^k(r, \beta, m)$. We consider only $\beta = 1$. For the special case involving NN ratios, we denote $P^1(r, \beta, 1) = P(r, \beta)$. The motivation for considering higher-order fluctuation statistics arises from a seminal result conjectured in Ref. [28] and proved by Gunson [29] for the case of circular ensembles of RMT.

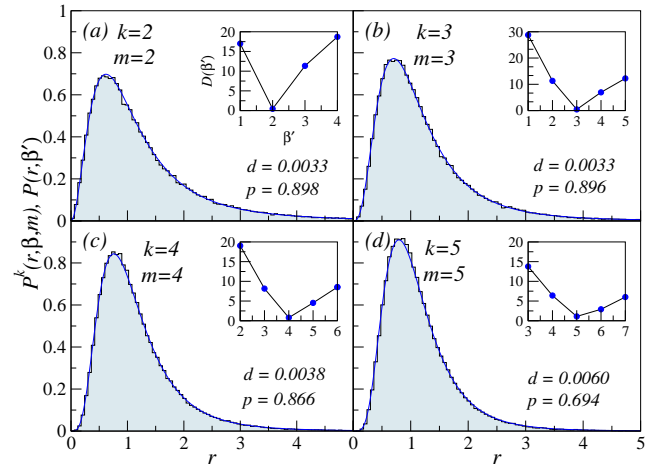


FIG. 2. Distribution of k -th order spacing ratios (histograms) for a superposition of m GOE spectra, each obtained by diagonalizing matrices of dimension $N = 40000$, shown for $m = 2$ to 5. The solid curve corresponds to $P(r, \beta')$, with $\beta' = k$. The insets show $D(\beta)$ whose minima correctly coincides with the expected value of m . Also shown are the test statistic (d) and the p -value (p) for the Kolmogorov-Smirnov test at a significance level of 0.05 for each case.

If two independent spectra from the circular orthogonal ensemble (COE) are superposed, upon integrating out every alternate eigenvalue, the joint probability distribution of the remaining eigenvalues follow circular unitary ensemble (CUE) statistics. In terms of higher-order measures, this result states that the second order statistics of two superposed COE spectra converges to NN statistics of CUE. This is reflected in the distribution of spacings and spacing ratios as well. In the limit of large matrix dimensions, this result holds for Gaussian ensembles too yielding $P^2(r, 1, 2) = P(r, 2)$ for two superposed spectra. This may be generalized for the superposition of m GOE spectra as

$$P^k(r, 1, m) = P(r, \beta'), \quad \text{where } \beta' = m = k, \quad (3)$$

implying that its k -th order spacing ratio distribution converges to NN statistics $P(r, \beta')$ with $\beta' = k$. Equation 3 is the main result of the paper. In contrast to this, irrespective of how many *uncorrelated* spectra are superposed corresponding to integrable systems, the k -th order spacing ratio distribution can be obtained (details in supplementary information [30]) as

$$P_P^k(r) = \frac{(2k-1)!}{[(k-1)!]^2} \frac{r^{k-1}}{(1+r)^{2k}}. \quad (4)$$

For $k = 1$, this reduces to $\frac{1}{(1+r)^2}$, the correct limit for the NN spacing ratio for uncorrelated spectra. We note that Eq. 3 is reminiscent of a scaling relation reported recently in Ref. [31].

For the superposition of $m = 2$ to 5 independent GOE spectra, validity of Eq. 3 is verified in Fig. 2. In this

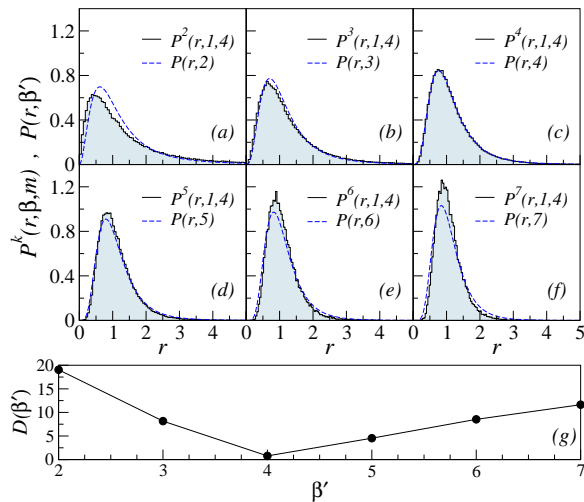


FIG. 3. (a-f) Computed k -th order spacing ratio distribution (histogram) for superposed spectra from four GOE matrices of order $N = 40000$. The broken line is $P(r, \beta' = k)$. Note that the best agreement is obtained only for $\beta' = k = 4$. (g) A plot of $D(\beta')$ vs. β' displays a clear minima for $\beta' = 4$ supporting the claim in Eq. 3.

figure, an excellent agreement is seen between histograms obtained from the computed eigenvalues of GOE matrices and the solid line representing $P(r, \beta' = k)$. For uncorrelated eigenvalues, a similar agreement with Eq. 4 is observed. In order to independently obtain a best quantitative estimate for β' in Eq. 3 for a given superposition of m spectra, we compute

$$D(\beta') = \sum_i |I_{obs}^m(r_i, 1, m) - I(r_i, \beta')|. \quad (5)$$

In this, $I_{obs}^m(r, 1, m)$ and $I(r, \beta')$ represents the cumulative distribution functions corresponding respectively to the observed histogram $P^k(r, 1, m)$ and the postulated function $P(r, \beta')$. If the minima of $D(\beta')$ occurs at, say, $\beta' = \beta_0$, then β_0 is the best estimate consistent with the observed data. As seen in the insets of Fig. 2, the minima in $D(\beta)$ coincides with the value of m , the number of superposed spectra.

A complete picture is revealed in Fig. 3 for a superposition of $m = 4$ independent GOE spectra, where the computed histogram for the k -th order ratio is shown for $k = 2$ to 7. Based on Eq. 3, we expect it to be consistent with $P(r, \beta' = 4)$. For each k , $P^k(r, 1, 4)$ is matched against the corresponding $P(r, \beta')$, and $D(\beta')$ is calculated. Both visually and quantitatively (the minima of $D(\beta')$ in Fig. 3(e)), best agreement is observed for $k = 4$, verifying the main result in Eq. 3. Significantly, for the superposed spectra, Eqs. 3-4 can be used to infer the correct nature of spectral fluctuations (level repulsion or clustering) and also to determine the number of superposed independent blocks for a random matrix or the number of diagonal blocks in the Hamiltonian matrix of

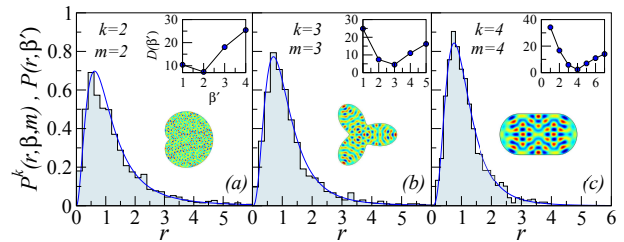


FIG. 4. HOSR distribution (histogram) for the billiards family computed by ignoring their symmetries. This corresponds to superposition of spectra from (a) $k = 2$, (b) $k = 3$ and (c) $k = 4$ irreps. The higher-order distributions are best described by $P(r, \beta')$ with $\beta' = k$ as dictated by Eq. 3. The insets display $D(\beta')$ and its minima corresponds to the correct number of irreps in the system. Also shown as inset is the shape of billiards with an arbitrarily chosen chaotic eigenstate to highlight its symmetry.

a complex quantum system, if the system is chaotic. Further, this result will be applied to chaotic systems possessing different symmetries, notably billiards and spin chains, and most importantly to the experimentally measured data of nuclear resonances.

First we consider quantum billiards, in which a free particle is confined in a cavity defined by a variety of boundaries [32], whose eigenspectrum is obtained by solving the Helmholtz equation with Dirichlet boundary conditions. They are popular models in Hamiltonian chaos and mesoscopic physics [33] and have experimentally-realized variants [34]. Modifying the boundary or shape of the billiard changes its symmetry properties and also drives it from integrability to chaos. For a billiard whose boundary is parameterized by $r(\phi) = r_0(1 + \epsilon \cos \phi)$, as ϵ varies from 0 to 1, the system transitions from integrable to chaotic dynamics. For $\epsilon = 0$, a circular billiard shown in Fig. 1(a) is obtained. This is an integrable system and its higher-order spacings are in agreement with Eq. 4 (See Ref. [30]). For $\epsilon = 1$, the so-called cardioid billiard is obtained [35], possessing two irreps due to reflection symmetry about the horizontal axis. Thus, eigenlevels obtained disregarding symmetry would correspond to a superposition of two GOE spectra. As anticipated by Eq. 3, its second order spacing ratio distribution $P^2(r, 1, 2)$ is consistent with $P(r, 2)$ (Fig. 4(a)). A billiard with three irreps, similar in shape to one that has been experimentally realized [36], is obtained by parametrizing its boundary as $r(\phi) = r_0(1 + 0.3 \cos(3\phi))$. This model, with symmetries ignored and after removing degeneracies arising from the two-dimensional irreps, corresponds to a superposition of three chaotic spectra and the best match for $P^3(r, 1, 3)$ is provided by $P(r, 3)$ (Fig. 4(b)). A chaotic billiard with four irreps is the well-studied Bunimovich stadium billiard [37] (shown in Fig. 4(c)). This has reflection symmetry about both x and y axes and, in accordance with Eq. 3, displays the best correspondence

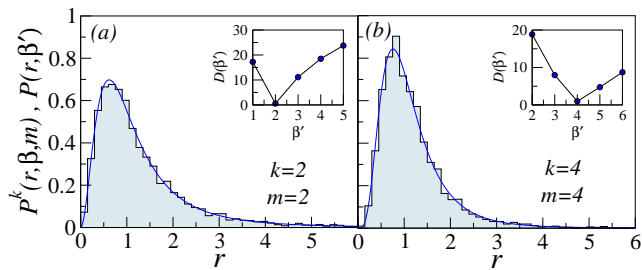


FIG. 5. HOSR distribution computed for the spin-1/2 chain Hamiltonian in Eq. 6, with (a) odd number of sites with two irreps and (b) even number of sites with four irreps. The insets show $D(r, \beta')$ and its minima identifies the number of irreps.

for $P^k(r, 1, 4)$ with $P(r, \beta')$ for $k = \beta' = 4$ (Fig. 4(c)). For all of these cases, insets in Fig. 4 show that the minima of $D(\beta')$ corresponds to $\beta' = k$, where k is the number of irreps. Thus, information about the fluctuation property and irreps can be obtained from higher-order fluctuation statistics.

Next, a spin-1/2 chain with the Hamiltonian [38]

$$H = \sum_{i=1}^{L-1} [J_{xy}(S_i^x S_{i+1}^x + S_i^y S_{i+1}^y) + J_z S_i^z S_{i+1}^z] + \eta \sum_{i=1}^{L-2} [J'_{xy}(S_i^x S_{i+2}^x + S_i^y S_{i+2}^y) + J'_z S_i^z S_{i+2}^z] \quad (6)$$

is considered, where L is the number of sites, J_{xy} and J_z are the NN coupling strengths in three directions (coupling along x and y being the same), and J'_{xy} and J'_z are the next NN coupling strengths. This system is integrable for $\eta = 0$ (as shown in Fig. 1 in Ref. [30]), and chaotic for $\eta \gtrsim 0.2$. The total spin in the z -direction, S_z , is conserved and the Hamiltonian is block diagonal in the S_z basis, with each block corresponding to a given value of S_z . However, other symmetries exist in the system. For odd number of sites (L_{odd}), on computing the HOSRs and comparing with corresponding $P(r, \beta')$, $k = \beta' = 2$ has the best match (Fig. 5(a)). But for even number of sites (L_{even}), HOSRs correspond to $k = \beta' = 4$ (Fig. 5(b)). This is because for L_{odd} or L_{even} , the parity operator (with eigenvalues ± 1) commutes with H , leading to two invariant subspaces in a given S_z block. For L_{even} , an additional rotational symmetry exists (with eigenvalues ± 1) for the corresponding operator giving rise to four irreps. The other parameters used in Figs. 5(a,b) are $J_{xy} = J'_{xy} = 1.0$, $J_z = J'_z = 0.5$, with $L_{even} = 14$ and $L_{odd} = 15$.

Even for systems whose Hamiltonian is not well-defined or unknown as in the case of complex nuclei, experimentally observed nuclear resonance data can be analyzed to characterize its fluctuation statistics and find its number of irreps. We consider a sequence of experimentally observed neutron resonances for Ta^{181} nucleus

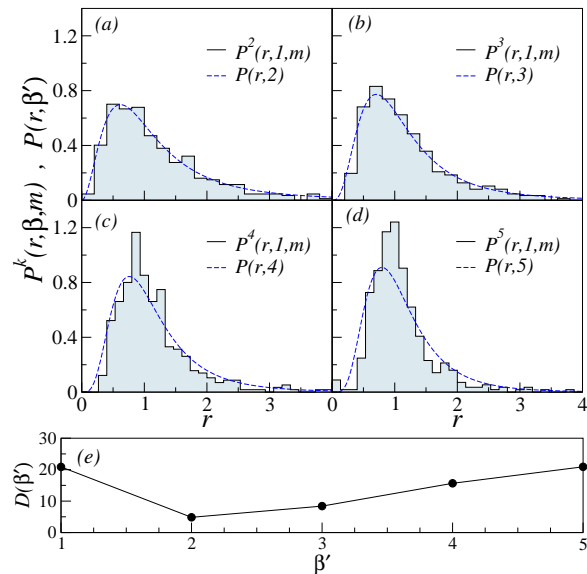


FIG. 6. (a-d) The k -th order spacing ratio distribution (histogram) for experimentally observed nuclear resonances for Tantalum (Ta^{181}), with the best correspondence observed for $k = 2$. The broken line is $P(r, \beta' = k)$. (e) $D(\beta')$ shows minima at $\beta' = 2$, reinforcing the validity of Eq. 3.

[39] whose NN spacing distribution is discussed in Ref. [14], and it does not match the Wigner surmise. On calculating higher-order ratio distributions, remarkably, Eq. 3 holds good for $k = 2$, and this is further confirmed by the minima of $D(\beta')$ for $\beta' = 2$ in Fig. 6. This indicates that two independent symmetry sectors might be present, and the resonances drawn from each symmetry sector displays level repulsion. This is indeed the case, as confirmed in Refs. [14, 39], that this measured sequence consists of a superposition of levels having angular momentum $J = 3$ and 4. When symmetry decomposed, they are in broad agreement with Wigner surmise. Clearly, for an arbitrary sequence of measured levels, HOSRs based on Eq. 3 can unambiguously identify the true fluctuation character and the number of symmetry sectors. Typically in experiments and sometimes even in simulations, the problem of missing levels is encountered [40] leading to incorrect identification of universality class of fluctuations and number of irreps. We tested the robustness of Eq. 3 to missing levels by deleting randomly chosen entries in a given sequence of levels from a superposition of GOE spectra. Upon computing $D(\beta')$ in each case (details in [30]), it was observed that Eq. 3 holds good even if up to 20 to 30% of the levels are removed as higher-order fluctuations are largely insensitive to randomly missing levels, which is a practical advantage of the method.

To summarize, quantum systems must be symmetry decomposed in order to reveal its true spectral fluctuation characteristics, implying that the fluctuations carry symmetry information, though extracting it unambiguously from NN fluctuation statistics is non-trivial. In

this work, it is demonstrated that the HOSR distributions can reveal, apart from the fluctuation characteristics, quantitative information about symmetry structure. For a superposition of k independent spectra, the central result (Eq. 3) relates the k -th order spacing ratio distribution for matrices with Dyson index $\beta = 1$ to the corresponding NN statistics with $\beta' = k$. For quantum systems in the classically chaotic limit and in the regime of applicability of Wigner-Dyson ensembles of RMT, this elegant relation determines the number of irreps (or diagonal blocks) present in a Hamiltonian matrix. This is exploited to analyze any arbitrary sequence of experimentally measured or computed levels, even if the system's Hamiltonian and symmetry structure are unknown. This technique requires neither unfolding nor free-parameter estimation, nor computation of cumbersome correlation or power spectral functions and hence straightforward to implement. Further, for uncorrelated eigenvalues, the HOSR distribution has been derived to be used as a test of integrability. These results have been demonstrated using disparate physical systems like quantum billiards, spin chains and experimentally measured nuclear resonances. In principle, this approach may be extended to weakly chaotic or mixed systems (outside of strict RMT regime) by considering a broader class of higher-order ratios and these results will be reported elsewhere.

* E-mail: harshini.t@gmail.com

† E-mail: santh@iiserpune.ac.in

- [1] T. Guhr, A. Muller-Groeling and H. A. Weidenmüller, Phys. Rep. **299**, 189 (1998).
- [2] C. E. Porter, *Statistical theories of spectra: fluctuations*. (Academic Press, New York 1965).
- [3] F. Haake, *Quantum signatures of chaos* (Springer Science & Business Media, Berlin Heidelberg 2013).
- [4] G. Akemann, J. Baik, and P. Di Francesco (eds.), *The Oxford handbook of random matrix theory*, (Oxford University Press, New York, 2011).
- [5] P. J. Forrester, *Log-Gases and Random Matrices (LMS-34)* (Princeton University Press, Princeton, NJ, 2010).
- [6] H. J. Stöckmann, *Quantum Chaos: An Introduction*, Cambridge U.P. (2000).
- [7] C. W. Beenakker, Rev. Mod. Phys. **69**, 731 (1997); Y. Alhassid, Rev. Mod. Phys. **72**, 895 (2000).
- [8] J. M. G. Gómez, K. Kar, V. K. B. Kota, R. A. Molina, A. Relaño, and J. Retamosa, Phys. Rep. **499**, 4-5 (2011).
- [9] N. Rosenzweig, and C. E. Porter, Phys. Rev. **120**, 1698 (1960); H. S. Camarda and P. D. Georgopoulos, Phys. Rev. Lett. **50**, 492 (1983).
- [10] L. Reichl, *The Transition to Chaos: Conservative Classical Systems and Quantum Manifestations*, Springer Science and Business Media (2013).
- [11] H. Hasegawa, and Y. Sakamoto, Progress of Theoretical Physics Supplement, **139**, 112 (2000); S. M. Nishigaki, Phys. Rev. E, **59**, 2853 (1999).
- [12] S. D. Geraedts, R. Nandkishore and N. Regnault, Phys. Rev. B, **93**, 174202 (2016).
- [13] H. A. Weidenmüller and G. E. Mitchell, Rev. Mod. Phys. **81**, 539 (2009).
- [14] T. A. Brody, J. Flores, J. B. French, P. A. Mello, A. Pandey and S. S. Wong, Rev. Mod. Phys. **53**, 385 (1981).
- [15] M. L. Mehta, *Random Matrices* (Academic Press, New York, 2004).
- [16] O. Bohigas, M. J. Giannoni and C. Schmidt, Phys. Rev. Lett. **110**, 064102 (1983).
- [17] D. Delande, and J. C. Gay, Phys. Rev. Lett. **57**, 2006 (1986); H. Friedrich and H. Wintgen, Phys. Rep. **183**, 37 (1989); C. Ellegard, T. Guhr, K. Lindemann, H. Q. Lorensen, J. Nygård and M. Oxborrow, Phys. Rev. Lett. **77**, 4918 (1996).
- [18] Harold U. Baranger and Pier A. Mello, Phys. Rev. Lett. **73**, 142 (1994); J. N. Bandyopadhyay and A. Lakshminarayan, Phys. Rev. Lett. **89**, 060402 (2002); Ph. Jacquod, H. Schomerus, and C. W. J. Beenakker, Phys. Rev. Lett. **90**, 207004 (2003).
- [19] S. Muller, S. Heusler, P. Braun, F. Haake, and A. Altland, Phys. Rev. Lett. **93**, 014103 (2004); *ibid*, Phys. Rev. E **72**, 046207 (2005).
- [20] M. V. Berry, and M. Tabor, Proc. R. Soc. Lond. A **356**, 1686 (1977).
- [21] M. V. Berry and M. Robnik, J. Phys. A, **17**, 12 (1984).
- [22] P. J. Forrester and E. M. Rains, Probability theory and related fields, **130**, 518 (2004).
- [23] T. Guhr and H.A. Weidenmüller, Chem. Phys. **146**, 21 (1990); L. Leviandier, M. Lombardi, R. Jost and J.P. Pique, Phys. Rev. Lett. **56**, 2449 (1986); J.B. French, V.K.B. Kota, A. Pandey, S. Tomsovic, Ann. Phys. (N.Y.) **181** (1988); R. A. Molina, J. Retamosa, L. Muoz, A. Relaño, and E. Faleiro, Phys. Lett. B, **644**, 25 (2007).
- [24] V. Oganessian, D. A. Huse, Phys. Rev. B **75**, 155111 (2007).
- [25] Y. Y. Atas, E. Bogomolny, O. Giraud, and G. Roux, Phys. Rev. Lett. **110**, 084101 (2013).
- [26] R. W. Robinet, Am. J. Phys. **64**, 440 (1996).
- [27] S. W. McDonald and A. N. Kaufman, Phys. Rev. Lett. **42**, 1189 (1979); G. Casati, F. Valz-Gris and I. Guarneri, Lett. Nuovo Cimento **28**, 279 (1980).
- [28] F. J. Dyson, J. Math. Phys. **3**, 1 (1962).
- [29] J. Gunson, J. Math. Phys. **3**, 4 (1962).
- [30] Supplemental Material
- [31] S. H. Tekur, U. T. Bhosale and M. S. Santhanam, Phys. Rev. B **98**, 104305 (2018).
- [32] M. Robnik, J. Phys. A: Math. Gen. **17**, 1049 (1984).
- [33] M. V. Berry, Eur. J. Phys. **2**, 91 (1981); M. V. Berry, Ann. Phys. **131**, 163 (1981).
- [34] J. Stein and H.-J. Stöckmann Phys. Rev. Lett. **68**, 2867 (1992); A. Kudrolli, V. Kidambi and S. Sridhar, Phys. Rev. Lett. **75**, 822 (1995); P. So, S. M. Anlage, E. Ott and R. N. Oerter, Phys. Rev. Lett. **74**, 2662 (1995); H. Schanze, H.-J. Stöckmann, M. Martínez-Mares, and C. H. Lewenkopf, Phys. Rev. E **71**, 016223 (2005); B. Dietz, T. Friedrich, H. L. Harney, M. Miski-Oglu, A. Richter, F. Schäfer, and H. A. Weidenmüller, Phys. Rev. Lett. **98**, 074103 (2007).
- [35] A. Bäcker, F. Steiner, and P. Stifter, Phys. Rev. E. **52**, 2463 (1995).
- [36] B. Dietz, A. Heine, V. Heuveline and A. Richter, Phys. Rev. E. **71**, 026703 (2005).
- [37] H. Alt, C. Dembowski, H.-D. Gräf, R. Hofferbert, H. Rehfeld, A. Richter, and C. Schmit, Phys. Rev. E **60**, 2851 (1999).

- [38] A. Gubin and L. F. Santos, *Am. J. Phys.* **80**, 246 (2012).
- [39] G. Hacken, R. Werbin, and J Rainwater, *Phys. Rev. C* **17**, 43 (1978).
- [40] M. Lawniczak, M. Bialous, V. Yunko, S. Bauch, and L. Sirko, *Phys. Rev. E* **98**, 012206 (2018); M. Bialous, V. Yunko, S. Bauch, M. Lawniczak, B. Dietz, and L. Sirko, *Phys. Rev. Lett.* **117**, 144101 (2016); O. Bohigas and M. P. Pato, *Phys. Lett. B* **595**, 171 (2004); F. J. Dyson and M. L. Mehta, *J. Math. Phys.* **4**, 701 (1963).

Supplemental Material

HIGHER ORDER DISTRIBUTION OF SPACING RATIOS FOR A SEQUENCE OF UNCORRELATED EIGENVALUES (EIGENVALUES OF INTEGRABLE QUANTUM SYSTEMS)

Analytical expression

For a given sequence of uncorrelated eigenvalues, $E_1 \leq E_2 \leq \dots \leq E_N$, the spacings between nearest neighbours is defined as $s_i = E_{i+1} - E_i, i = 1, 2, \dots, N$. The distribution of these spacings is of the form $P(s) = e^{-s}$, and hence distributions of spacings and spacing ratios for integrable quantum systems are termed Poissonian.

The ratios of nearest neighbour spacings for these systems are defined as $r_i = s_{i+1}/s_i, i = 1, 2, \dots, N$, and the distribution of these ratios is of the form $P(r) = 1/(1+r)^2[1]$.

Ratios of higher order spacings may be defined as

$$r_i^{(k)} = \frac{s_{i+k}^{(k)}}{s_i^{(k)}} = \frac{E_{i+2k} - E_{i+k}}{E_{i+k} - E_i}, \quad i, k = 1, 2, 3, \dots \quad (7)$$

To obtain a form for the distribution of $r^{(k)}$, the higher order spacings may be expressed in terms of nearest neighbour spacings as

$$\begin{aligned} s_i^{(k)} &= E_{i+k} - E_i \\ &= E_{i+k} - E_{i+k-1} + E_{i+k-1} - E_{i+k-2} + \dots + E_i \\ &= s_k + \dots + s_{i+1} + s_i. \end{aligned} \quad (8)$$

Then the distribution of $s_i^{(k)}$ may be calculated as the distribution of a sum of k random variables s_i , each of which is distributed as $P(s) = e^{-s}$. For simplicity, $s_i^{(k)}$ is denoted as z below. The distribution of z is given by

$$P(z) = \frac{e^{-z} z^{k-1}}{(k-1)!} \quad (9)$$

Then the distribution of higher order spacing ratios is simply the distribution of the quotient of two random variables, each of which is distributed as Eq. 9. This distribution may be calculated as

$$P_P^{(k)}(r) = \int |z| P(rz) P(z) dz \quad (10)$$

Substituting for $P(z)$ and $P(rz)$ from Eq. 9,

$$\begin{aligned} P_P^{(k)}(r) &= \int_0^\infty |z| \frac{e^{-rz} (rz)^{k-1}}{(k-1)!} \frac{e^{-z} z^{k-1}}{(k-1)!} dz \\ &= \frac{r^{k-1}}{(k-1)!^2} \int_0^\infty z^{2k-1} e^{-z(r+1)} dz. \end{aligned} \quad (11)$$

This can be evaluated in terms of the incomplete gamma function $\Gamma(x)$ as

$$\begin{aligned} P_P^{(k)}(r) &= \frac{\Gamma(2k)}{(k-1)!^2} \frac{r^{k-1}}{(1+r)^{2k}} \\ &= \frac{(2k-1)!}{((k-1)!)^2} \frac{r^{k-1}}{(1+r)^{2k}}. \end{aligned} \quad (12)$$

For $k = 1$, it reduces to the familiar form

$$\frac{1}{(1+r)^2}.$$

For $k = 2$,

$$P_P^{(2)}(r) = \frac{6r}{(1+r)^4}, \quad (13)$$

for $k = 3$,

$$P_P^{(3)}(r) = \frac{30r^2}{(1+r)^6}, \quad (14)$$

and for $k = 4$,

$$P_P^{(4)}(r) = \frac{140r^3}{(1+r)^8}. \quad (15)$$

Comparison of analytical form of $P_P^{(k)}(r)$ with results from physical systems

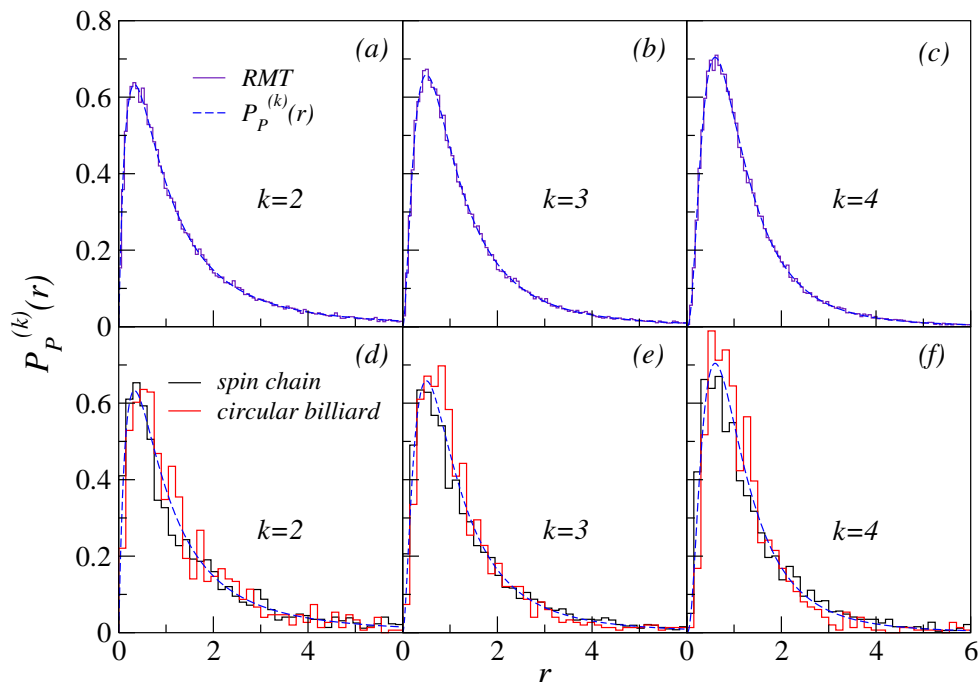


FIG. 7. Higher order spacing ratio distributions for $k = 2$ to 4 , for uncorrelated eigenvalues (upper panel, indigo), circular billiards (lower panel, red) and integrable spin chain obtained by setting $\eta = 0$ in Eq. 6 of the main paper (lower panel, black). The corresponding analytical result (Eq. 4 in the main paper) is also shown in all cases (upper and lower panels, broken blue curve).

EFFECT OF MISSING LEVELS

The effect of missing levels in a given sequence of superposed spectra is studied by randomly deleting a fixed percentage of levels, and then calculating higher order spacing ratios, from a superposition of GOE spectra of dimension $N = 40000$. In each case, $D(\beta')$ is calculated, and the value of β' corresponding to the minima of $D(\beta')$ corresponds to the best fit.

Fig. 8 shows the value of β' (evaluated in steps of 0.1) plotted against the percentage of missing levels, when $P^k(r, 1, m)$ is evaluated for a superposition of m GOE spectra, where $m = 2$ (blue) and $m = 4$ (red). According to

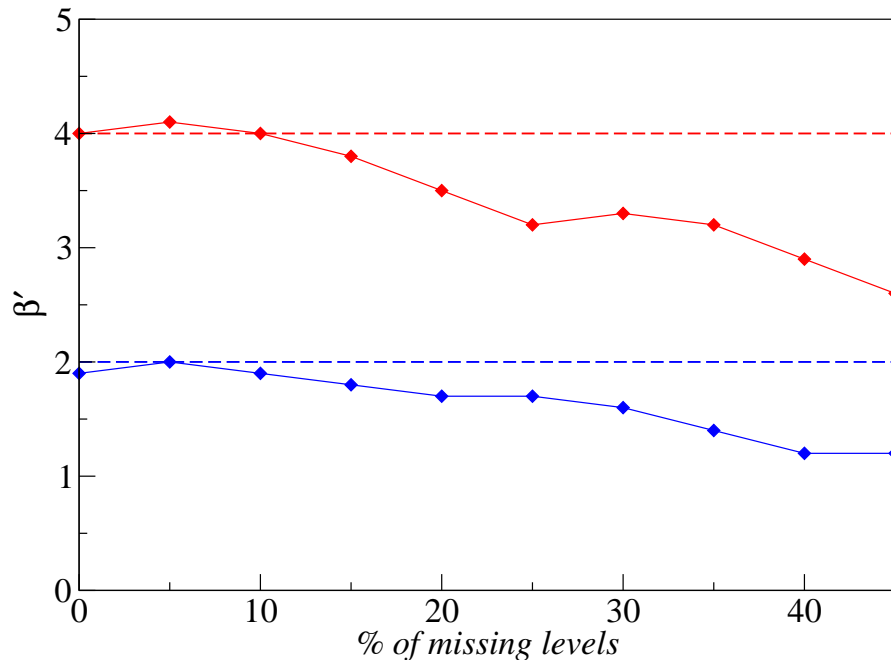


FIG. 8. β' (for which $D(\beta')$ is minimum) as a function of percentage of missing levels obtained by evaluating the second (fourth) order spacing ratio distribution for a superposition of two(four) GOE spectra, plotted in red(blue). The dashed lines correspond to the value of β' as predicted by Eq. 4 of the main paper.

Eq. 4 of the main paper, namely, $P^k(r, 1, m) = P(r, \beta')$, where $\beta' = m = k$, the expected value of β' is 2 (for $k = 2$) and 4 (for $k = 4$) respectively, given by the blue and red dashed lines in Fig 8. It may be observed that assuming even a 10% fluctuation in the numerical evaluation of β' , a significant deviation from the predicted β' occurs only when about 20% of the levels are missing. A similar behavior was seen for spin chains with 2 and 4 irreps as well (not shown).

* E-mail: harshini.t@gmail.com

† E-mail: santh@iiserpune.ac.in

[1] Y. Y. Atas, E. Bogomolny, O. Giraud, and G. Roux, Phys. Rev. Lett. **110**, 084101 (2013).